

Structures of Strontium Selenite and Strontium Selenide Aluminate Sodalites and the Relationship of Framework Structure to Vibrational Spectra in Aluminate Sodalites

Matthew E. Brenchley and Mark T. Weller*

Department of Chemistry, The University of Southampton, Southampton, SO9 5NH, U.K.

Received January 20, 1993. Revised Manuscript Received April 27, 1993

The structures of both $\text{Sr}_8[\text{AlO}_2]_{12}(\text{SeO}_3)_2$ and its reduced product $\text{Sr}_8[\text{AlO}_2]_{12}(\text{Se})_2$ have been determined using profile refinements of powder neutron diffraction data. Both crystallize with the simple body centered cubic sodalite structure with strontium showing a tetrahedral coordination around $\text{SeO}_3^{2-}/\text{Se}^{2-}$, and selenite showing 24-fold disordering giving rise to a partially occupied distorted cuboctahedron comprising 24 identical deformed SeO_3 trigonal pyramids. The infrared spectra of aluminate sodalites as a function of cage dimensions are discussed.

Introduction

Incorporation of anions into framework structures provides a method of dispersing and stabilizing small inorganic species. Such materials include the well known ultramarines, containing S_2^- and S_3^- , which are widely used as pigments. Recent attention to anions in zeolite frameworks has included work directed to forming semiconductor nanoparticles with the encapsulation of S^{2-} and Se^{2-} with divalent cations.

Sodalites of general formula $[\text{M}_n]^{8+}\{\{\text{TO}_2\}_q\}^{6-}\cdot[\text{X}_y]^{2-}$ have been shown to form for a wide variety of chemical compositions.¹⁻³ The structure is composed of corner sharing TO_4 tetrahedra (T = Si, Al, Be, P, B, Zn, Ga etc) in four and six rings giving the β -cage unit adopted by zeolites. The β -cages are linked directly through the six membered rings. The metals, M, adopt a tetrahedral geometry around the central anion, X, and coordinate to both the anion and the oxygens in the six ring (as shown in Figure 1). Many different metals (M = Li^+ , Na^+ , K^+ , Mg^{2+} , Ca^{2+} , Sr^{2+} , Ba^{2+} , Ag^+ , Tl^+ , etc) and anions (X = Cl^- , Br^- , I^- , SCN^- , NO_2^- , NO_3^- , SO_4^- , MnO_4^- , CrO_4^{2-} , ClO_4^- , $\text{C}_2\text{O}_4^{2-}$, CO_3^{2-} , etc.) of various sizes and geometries can be accommodated by a partial collapse of the structure which is performed by tilting of the tetrahedra out of their normal planes and by deviation from perfect tetrahedral geometries.

Several methods have been used for sodalite synthesis of which the most versatile are solution/hydrothermal methods.¹ Other less adaptable but equally effective methods are high-temperature sintering⁴ and the structure conversion technique.⁵ Within the structure the linking of six membered rings allows post phase reactions, which involve ions with small ionic radii, to occur with ease, such as metal ion exchange and anion decomposition, e.g., S_2^- and S_3^- formation from SCN^- in the production of ultramarine.⁶

The aluminate sodalites of general formula $\text{M}_8[\text{AlO}_2]_{12}\cdot\text{X}_2$ (M = Ca^{2+} , Sr^{2+} , Cd^{2+} ; X = SO_4^{2-} , WO_4^{2-} , CrO_4^{2-} ,

MoO_4^{2-} , S^{2-}) disobey Lowenstein's⁷ rule of aluminium avoidance. Structural studies on these sodalites by Depmeier⁸⁻¹⁰ have shown that the basic β -cage unit remains and that the tetrahedral anions are located at the center of the β -cage. At 300 K $\text{Ca}_8[\text{AlO}_2]_{12}(\text{WO}_4)_2$ sodalite has been shown to possess an orthorhombic super structure caused by specific orientations of the WO_4^{2-} group which aligns the W-O bond toward a cage oxygen in the four ring. This repels the cage giving rise to the super structure comprising of eight β -cage units. If $\text{Ca}_8[\text{AlO}_2]_{12}(\text{WO}_4)_2$ is heated above 656 K, the superstructure is lost and the simple body-centered cubic sodalite structure is observed; in the high-temperature phase the WO_4^{2-} group can adopt six possible orientations (two in each of three mutually perpendicular axis) without preference.

In a recent study by the authors¹¹ it was found that sulfate-bearing aluminate sodalites could be reduced to yield sulfide aluminate sodalites which are of interest due to their short M-S bond distance and consequent charge-transfer process between the two. In a recent study¹² CdS and PbS as M_4S_4 clusters were introduced into zeolite cages and were found to have similar charge transfer bands in the UV as the bulk materials and hence are potential semiconductors. The synthesis of the new chalcogenide aluminate sodalites has stimulated us to prepare new materials of this family, and in this article we report the synthesis and structure of two new members of this family. The framework geometry in aluminosilicate sodalites is reflected in the vibrational spectrum with good correlation between bond angles and frequencies. With the increasing number of aluminate sodalites we present similar correlative data for these materials.

Experimental Section

Kondo¹³ and later Depmeier¹⁴ explored aluminate sodalite synthesis at high temperature by a solid-state sintering reaction of the metal oxide/salt and alumina. $\text{Sr}_8[\text{AlO}_2]_{12}(\text{SeO}_3)_2$ was

- (1) Barrer, R. M.; Cole, J. F. *J. Chem. Soc. A* 1970, 1516.
- (2) Taylor, D.; Henderson, C.M.B. *Phys. Chem. Miner.* 1978, 2, 325.
- (3) Weller, M. T.; Wong, G. *J. Chem. Soc., Chem. Commun.* 1988, 1103.
- (4) Prener, J. S.; Ward, R. *J. Am. Chem. Soc.* 1988, 72, 2780.
- (5) Chang, I. *J. Electrochem. Soc.* 1974, 121 (6), 815.
- (6) Hund, F. *Z. Anorg. Allg. Chem.* 1984, 511, 225.

- (7) Lowenstein, W. *Am. Miner.* 1954, 39, 92.
- (8) Depmeier, W. *Acta Crystallogr.* 1988, B44, 201.
- (9) Depmeier, W. *Acta Crystallogr.* 1987, C43, 2251.
- (10) Depmeier, W. *Acta Crystallogr.* 1984, C40, 226.
- (11) Brenchley, M. E.; Weller, M. T. *J. Mater. Chem.* 1992, 2, 1003.
- (12) Herron, N.; Wang, Y.; Eddy, M. E.; Stucky, G. D.; Fox, D. E.; Moller, K.; Bein, T. *J. Amer. Chem. Soc.* 1989, 111, 530.
- (13) Kondo, R. *Yogyo Kyokai Shi* 1965, 71, 1.
- (14) Depmeier, W. *Kristall. Technik* 1972, 7, 229.

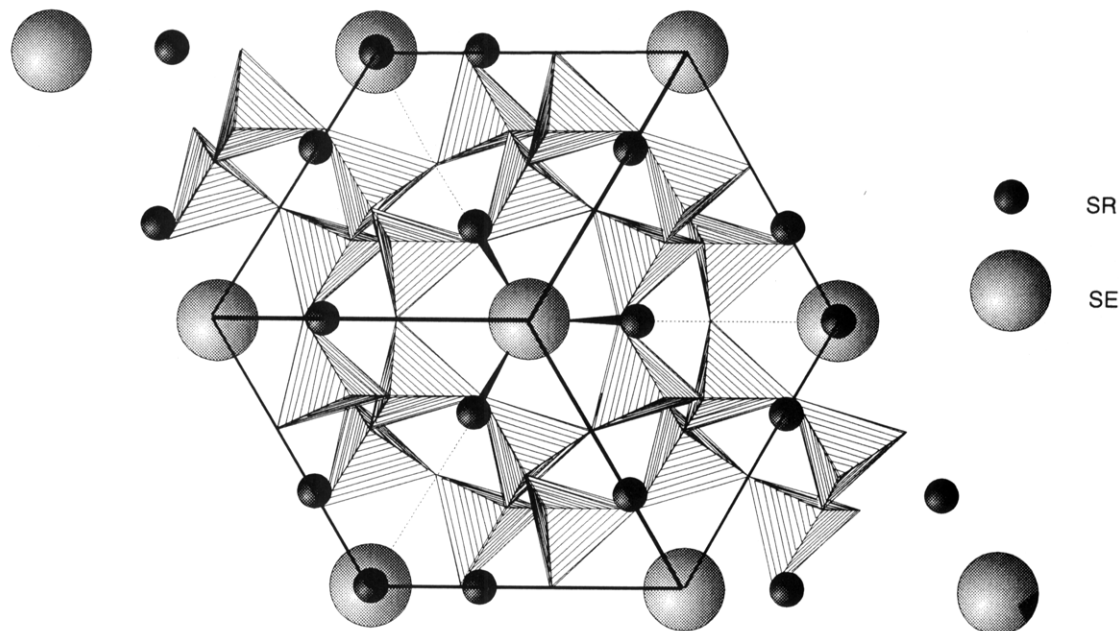


Figure 1. Partially collapsed sodalite structure viewed along the six ring channel. Relative positions of Sr and Se are shown.

prepared by firing a finely ground stoichiometric mixture of SrCO_3 , SrSeO_3 , and Al_2O_3 in air at 1100°C for 24 h with periodic regrinding. The product crystallized as a fine white powder which was shown to be a single cubic phase with $a = 9.4315(1)$ Å by powder X-ray diffraction.

$\text{Sr}_8[\text{AlO}_2]_{12}(\text{Se})_2$ was prepared by reducing $\text{Sr}_8[\text{AlO}_2]_{12}(\text{SeO}_3)_2$ in a stream of $\text{H}_2(\text{g})$ at 850°C for 8 h. The measured weight loss of 5.88% is in good agreement with the expected value of 5.77%:



The product crystallized as a light yellow powder which was shown to be a single cubic phase with $a = 9.3048(1)$ Å by powder X-ray diffraction.

Infrared spectra were obtained for both compounds on a Perkin-Elmer FT-IR 1710 spectrometer with a 3600 data station as pressed KBr disks. On reduction of $\text{Sr}_8[\text{AlO}_2]_{12}(\text{SeO}_3)_2$ the peak attributable to the ν_3 asymmetric stretching vibration of SeO_3^{2-} at 750 cm^{-1} disappeared as can be seen in Figure 2.

Structure Determination

Time-of-flight neutron diffraction data were obtained for $\text{Sr}_8[\text{AlO}_2]_{12}(\text{SeO}_3)_2$ at both 295 and 5 K and for $\text{Sr}_8[\text{AlO}_2]_{12}(\text{Se})_2$ at 295 K over the range $3.08\text{--}0.568$ Å d spacing. All patterns could be indexed on a body centered cubic structure with systematic absences giving the space group $I\bar{4}3m$, the group adopted by sodalites crystallizing with no ordering of the tetrahedral framework sites. Reitveld refinements were performed in this space group using the Fortran program TF14LS.¹⁵

Starting models taken from Brenchley and Weller¹¹ were used for all three refinements with selenium assigned to the 2a (0,0,0) site, strontium on the 8c (x,x,x) $x \approx 0.22$ site, aluminium on the 12d ($1/4, 1/2, 0$) site and the cage oxygen on the 24g (x,x,z) $x \approx 0.15, z \approx 0.47$. For the selenites the 24g (x,x,z) $x \approx 0.38, z \approx 0.51$ site was chosen for the selenite oxygen (O_{Se}) allowing good coordination to the cage and metals, as had been reported by Depmeier when refining the similar chromate sodalite.⁹ Neutron scattering lengths for the above elements were taken as Se 0.797, Sr 0.702, Al 0.3449, and O 0.5803×10^{-12} cm. Data were normalized and corrected for sample absorption. The refinement

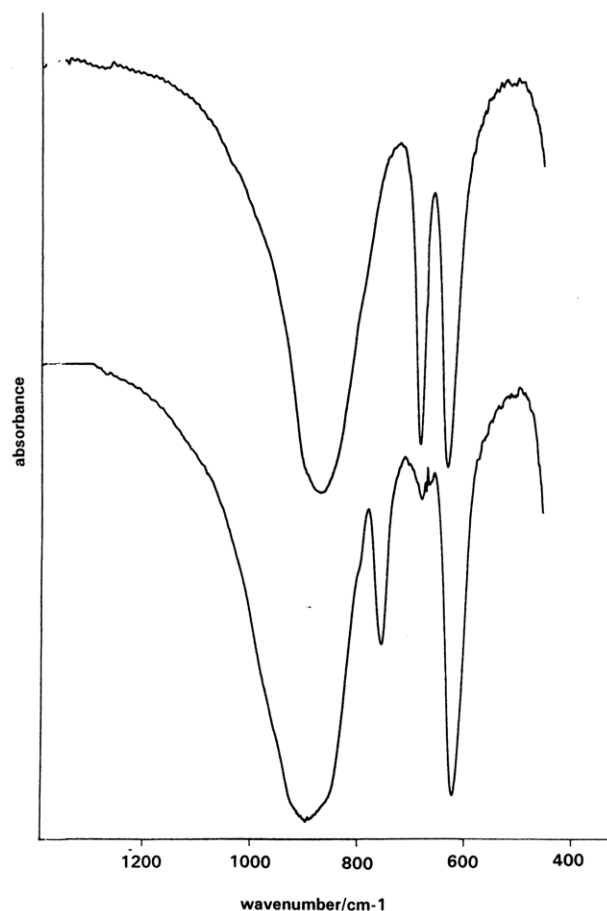


Figure 2. Infrared spectra of $\text{Sr}_8[\text{AlO}_2]_{12}(\text{Se})_2$ (upper) and $\text{Sr}_8[\text{AlO}_2]_{12}(\text{SeO}_3)_2$ (lower) showing the loss of the SeO_3^{2-} ν_3 asymmetric mode at 750 cm^{-1} .

proceeded well with scale factor, cell constant, and a ten-point polynomial background refined in the initial stages. All variable atom positions and peak-shape parameters were then refined with isotropic temperature factors added for all atoms subsequently. Final stages of the refinement included anisotropic temperature factors for all atoms in $\text{Sr}_8[\text{AlO}_2]_{12}(\text{Se})_2$ and for Sr and O_{Se} in $\text{Sr}_8[\text{AlO}_2]_{12}(\text{SeO}_3)_2$

(15) David, W. I. F.; Ibberson, R. M.; Matthewman, J. C. *Profile Analysis of Neutron Powder Diffraction Data at ISIS*.

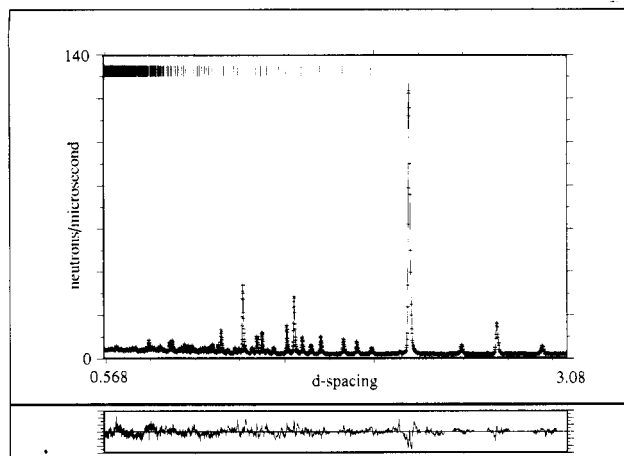


Figure 3. Profile fit to the powder neutron data from $\text{Sr}_8[\text{AlO}_2]_{12}(\text{Se})_2$. Crosses are observed data with the calculated profile as the solid line. The lower line is difference plot and tick marks show positions of allowed reflections.

Table I

atom	X	Y	Z	$B_{\text{iso/eq}}$
(a) Final Atomic Positions for $\text{Sr}_8[\text{AlO}_2]_{12}(\text{Se})_2$ at 295 K				
Al	0.25	0.5	0.0	0.269(20)
O	0.15411(5)	0.15411(5)	0.45374(17)	0.866(13)
Sr	0.19180(5)	0.19180(5)	0.19180(5)	0.803(12)
Se	0.0	0.0	0.0	1.294(23)
$a = 9.30357(3)$ Å, $R_{\text{wp}} = 1.90$, $R_{\text{ex}} = 1.52$				
(b) Final Atomic Positions for $\text{Sr}_8[\text{AlO}_2]_{12}(\text{SeO}_3)_2$ at 295 K				
Al	0.25	0.5	0.0	0.461(27)
O	0.15826(10)	0.15826(10)	0.4949(5)	0.975(21)
Sr	0.2435(8)	0.2435(8)	0.2435(8)	2.79(11)
Se	0.0	0.0	0.0	3.30(8)
O _{Se-1/4 occupied}	0.3795(8)	0.3795(8)	0.4944(39)	3.58(18)
$a = 9.43415(3)$ Å, $R_{\text{wp}} = 4.74$, $R_{\text{ex}} = 1.28$				
(c) Final Atomic Positions for $\text{Sr}_8[\text{AlO}_2]_{12}(\text{SeO}_3)_2$ at 5 K				
Al	0.25	0.5	0.0	0.118(29)
O	0.15809(11)	0.15809(11)	0.49208(30)	0.567(22)
Sr	0.2414(5)	0.2414(5)	0.2414(5)	1.74(10)
Se	0.0	0.0	0.0	2.54(8)
O _{Se-1/4 occupied}	0.3811(6)	0.3811(6)	0.5131(14)	2.64(33)
$a = 9.41785(3)$ Å, $R_{\text{wp}} = 2.41$, $R_{\text{ex}} = 0.72$				

Table II. Derived Bond Distances and Angles

bond distance (Å) angle (deg)	$\text{Sr}_8[\text{AlO}_2]_{12}(\text{Se})_2$		$\text{Sr}_8[\text{AlO}_2]_{12}(\text{SeO}_3)_2$	
	at 295 K	at 5 K	at 5 K	at 295 K
Al-O	1.7426(8)	1.724(3)	1.726(4)	
Sr-O	2.4869(16) × 3	2.609(11) × 3	2.630(17) × 3	
Sr-Se	3.0926(16) × 3	2.703(11) × 3	2.687(17) × 3	
Se-O _{se}	3.0907(8)	1.588(15)	1.608(38)	
Sr-O _{se}		2.899(23) 3 × 1/4	2.781(48) 3 × 1/4	
O-O _{se}		3.165(23) 3 × 1/4	2.983(48) 3 × 1/4	
O-Al-O × 2	118.41(8)	119.70(15)	119.86(16)	
O-Al-O × 4	105.19(8)	104.61(15)	104.54(16)	
Al-O-Al	141.40(6)	149.90(10)	150.14(10)	
φ tilt angle	16.71(2)	2.87(11)	1.84(17)	
O _{se} -Se-O _{se} × 1		90.3(7)	90.1(10)	
O _{se} -Se-O _{se} × 2		119.8(7)	120.0(10)	

giving final atomic positions and $B_{\text{iso/eq}}$ shown in Table I (Figure 3).

Results and Discussion

From the refined atomic positions bond distances and angles were calculated and are shown in Table II. In $\text{Sr}_8[\text{AlO}_2]_{12}(\text{Se})_2$ (shortened to SRSE hereafter) as for the true sodalite $\text{Na}_8[\text{AlSiO}_4]_6\text{Cl}_2$ the anion is tetrahedrally coordinated to the metal. The Sr-Se bond distance

(3.0907(8) Å) is slightly shorter than for the simple binary material (3.123 Å) which possesses the simple rock salt structure and hence has a octahedral coordination to the metal. A shorter metal-chalcogenide distance was also observed for $\text{Ca}_8[\text{AlO}_2]_{12}(\text{S})_2$ and $\text{Sr}_8[\text{AlO}_2]_{12}(\text{S})_2^{11}$ and is caused by a smaller effective ionic radii of S^{2-} and Se^{2-} in IV coordination as compared to the more common VI coordination. In $\text{Sr}_8[\text{AlO}_2]_{12}(\text{SeO}_3)_2$ (shortened to SRSEO for convenience) there is no direct interaction between the metals and Se, but coordination of the anion is performed by various orientations of the selenite oxygens (O_{se}) with the metals. This topic is dealt with in more detail later in this discussion.

In SRSE it can be seen that the strontium coordinates to the framework oxygens with two significantly different bond lengths caused by a partial collapse of the cage. This gives a nearest neighbour threefold coordination of Sr to the cage plus a fourth bond to Se^{2-} , placing it in a distorted tetrahedral coordination with weak interactions to a further three cage oxygens. However, in SRSEO the cage is more open with Sr nearly in the center of the six ring. This gives rise to sixfold coordination of Sr to the cage plus six further 1/4 interactions (on average) with the anion oxygens in the β-cages either side of the six ring giving a 7.5-fold coordination.

Al-O bond distances in all three refinements are in good agreement with other aluminate sodalites but with a small increase in SRSE in comparison to SRSEO. This trend has also been observed in other aluminate sodalites, the average Al-O bond distance for $\text{S}^{2-}/\text{Se}^{2-}$ containing sodalites is ≈ 1.745 Å where as for $\text{SeO}_3^{2-}/\text{CrO}_4^{2-}$ - WO_4^{2-} -containing sodalites the Al-O distance is typically ≈ 1.726 Å.

Most of the cell collapse is performed by large variations in the Al-O-Al bond angle which can take values between 120–160° and is generally larger than for aluminosilicate sodalites whose bond ionicities are less. The level of collapse of the aluminate cage can be described by several values discussed in much more detail by Depmeier.¹⁶ Of importance are α and α' which are the tetrahedral distortion angles for the O-Al-O angles in the AlO_4 tetrahedron, which can distort considerably from the perfect 109.48° angle. The more important term in defining the cell collapse is the tilt angle ϕ which describes how much the tetrahedra have tilted out of their 4 axis. ϕ can hold values from 0 to 35° and which if 0 produces a centrosymmetric fully expanded sodalite in the space group $Im\bar{3}m$. On cooling SRSEO from 295 to 5 K, it can be seen that the cell collapse is performed by tilting the AlO_4 tetrahedra from 1.84° to 2.87° as well as a reduction in Al-O bond length. In general for aluminate sodalites changes in the cell dimension are reflected in modification of the geometry of the AlO_4 tetrahedra. That is as a decreases the Al-O-Al angle decreases, the tetrahedral distortion angles α and α' tend toward 109.48° and the tilt angle ϕ becomes larger.

By choosing the 24g (x, x, z) $x \approx 0.38$, $z \approx 0.51$ site for O_{se} the selenite group produced represents a range of orientations over the vertices of a cuboctahedron distorted towards a truncated tetrahedron centered on $(1/2, 1/2, 1/2)$. The selenite coordination also allows equal probabilities for the SeO_3^{2-} trigonal pyramids to be in any of 24 orientations generated by the cuboctahedron, and hence

(16) Depmeier, W. *Acta Crystallogr.* 1984, B40, 185.

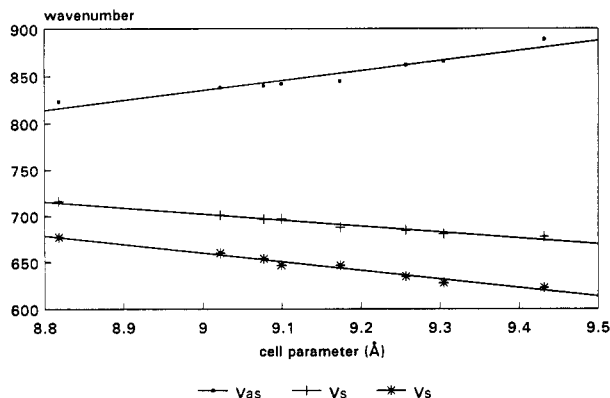


Figure 4. Plot of framework vibrational frequencies vs cell dimension for aluminate sodalites in Table III.

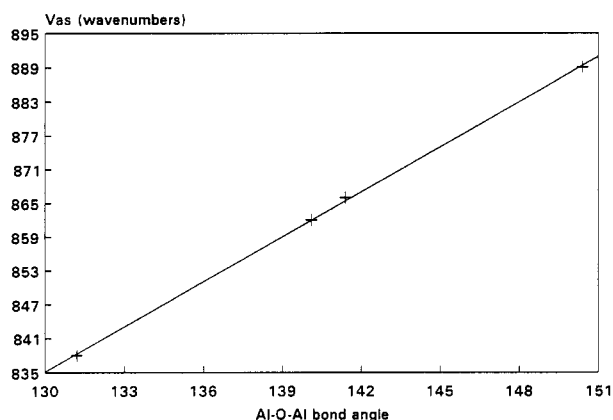


Figure 5. Plot of framework asymmetric vibration ν_{as} vs framework Al-O-Al angle for aluminate sodalites in Table III.

Table III. Measured Cell Parameters and Vibrational Frequencies for Aluminate Sodalites

sodalite	ν_{as} (cm ⁻¹)	ν_s (cm ⁻¹)	a (Å)	Al-O-Al (°)
Sr ₃ [AlO ₂] ₁₂ (SeO ₃) ₂	889	678, 623	9.434	150.4
Sr ₃ [AlO ₂] ₁₂ Se ₂	866	681, 628	9.303	141.4
Sr ₃ [AlO ₂] ₁₂ S ₂	862	685, 635	9.257	140.1
Ca ₃ [AlO ₂] ₁₂ (SeO ₃) ₂	845	688, 647	9.174	
Cd ₃ [AlO ₂] ₁₂ (SO ₄) ₂	842	697, 647	9.099	
Ca ₃ [AlO ₂] ₁₂ Se ₂	840	697, 654	9.077	
Ca ₃ [AlO ₂] ₁₂ S ₂	838	701, 660	9.022	131.2
Cd ₃ [AlO ₂] ₁₂ S ₂	823	716, 677	8.818	

no superstructures (caused by ordering of the anions) are found. These orientations give a coordination of O_{Se} to the metal consisting of three O_{Se}-Sr interactions which are 1/4 occupied and three O_{Se}-O_{cage} interactions of 2.952 Å, which are commonly seen in M²⁺SeO₃²⁻ type compounds. The internal angles of the selenite trigonal pyramids are apparently quite different from those observed in other simple M²⁺SeO₃²⁻ type compounds. Normally all three O-Se-O angles are of the order of 110°

but in the sodalite angles of 2 × 120.0° and 1 × 90.1° are observed. However, it is thought that this is a result of the limitations of the refinement in which the least number of variables is used to yield a reasonable model for the selenite group. A better model for the selenite group would probably involve distributing each of the three oxygens over a 48-fold general (x,y,z) site. Under such a model with 48 × 3 possible selenite oxygens in the unit cell, refinement of these positions would be impossible.

On cooling SRSEO, considerable changes in the selenite geometry and orientations as a result of ordering may have been expected. This, however, was not the case and the main feature of cooling the sample was an decrease in the Se-O_{Se} bond distance from 1.608 to 1.588 Å. The structure of SrSeO₃ is unknown and no direct comparison of Sr/SeO₃ interactions can be made. However values between 1.59 and 1.76 Å have been observed for the Se-O distance in selenites.^{17,18}

Vibrational Spectra of Aluminate Sodalites

The infrared absorption spectra of many sodalites have been studied by Henderson and Taylor.¹⁹ They found that three strong absorptions were observed for the T-O-T unit with one strong broad band at 800-1000 cm⁻¹ from the asymmetric stretch (ν_{as}) and two much more well defined peaks from symmetric vibrations (ν_s) seen between 500 and 800 cm⁻¹. Plots of ν_{as} and ν_s against the cell parameter were linear for all sodalite cage types. In addition to the two sodalites whose structures are discussed in detail above the authors have synthesized a range of aluminate sodalites as summarised in Table III together with their lattice parameters. Figure 4 plots ν_{as} and ν_s versus a for these sodalites plus those values for SRSE and SRSEO. It can be seen that the linear relationship of ν_{as} and ν_s versus a holds for aluminate sodalites over a wide range of cell parameters (8.82-9.43 Å) and that predicted values of 866, 683, and 632 cm⁻¹ for SRSE and 881, 673, and 619 cm⁻¹ for SRSEO compare very well with the observed values of SRSE 866, 681, and 628 cm⁻¹ SRSEO 889, 678, and 623 cm⁻¹. Also found was a linear relationship between the Al-O-Al bond angle and ν_{as} , Figure 5, which is predictively better for values of ν_{as} than the cell parameter relationship (SRSE 866 cm⁻¹, SRSEO 891 cm⁻¹). Further studies of these materials including ²⁷Al MAS-NMR work are in progress.

Acknowledgment. We would like to thank the University of Southampton and A.E.A. Technology Winfrith for a partial studentship support for M.E.B.

(17) Valkonen, J.; Leskela, M. *Acta Crystallogr.* 1978, B34, 1323.

(18) Jones, P. G.; Sheldrick, G. M.; Schwarzmann, E.; Vielmader, A. *Z. Naturforsch* 1983, 38B, 10.

(19) Henderson, C. M. B.; Taylor, D. *Spectrochim. Acta* 1979, 35A, 929.